Molecular Dynamic Simulation of the Structure of Water in the Vicinity of a Solvated Ion

M. Rao†ⁿ and B. J. Berne*

Department of Chemistry, Columbia University, New York, New York 10027 (Received: October 30, 1980)

Molecular dynamic simulations are used to study how water relaxes around an ion immediately after ionization. It is found that the rotational relaxation in the first and second coordination shells is much faster than would be expected on the basis of equilibrium time correlation functions. It is shown that, immediately after ionization, the local temperature increases dramatically, and the resulting "hot spot" dissipates very slowly on the time scale of the structural relaxation. In addition to this, molecular dynamics is used to study the equilibrium structure of water around various "ions" in "bulk" water and in clusters. It is found that the local structure is not affected by the boundary conditions.

I. Introduction

In recent years molecular dynamics and Monte-Carlo simulations have provided a very revealing picture of the structural and dynamical features of aqueous solutions.[1] In several recent publications, we have used these techniques to explore the hydrophobic effect.[2] In this paper we use molecular dynamics to study the properties of a system containing a single ion dissolved in water.

In the first part of the study, a neon atom is aged (equilibrated) in H_2O and the structure of the solution is determined. The "neon" atom is then instantaneously ionized to form a positive ion. This ion exerts a strong electrostatic field on the H_2O molecules, and these in turn respond by relaxing to new orientations and positions. During this subsequent relaxation the energy is conserved, the potential energy decreases, and the kinetic energy and hence the temperature must increase. Because the system is periodic (or isolated) and small, there is no mechanism for energy dissipation, and therefore the relaxation process is accompanied by a substantial temperature increase. This study shows how the radial distribution of various quantities changes in time (relax) after the initial charging (ionization) of the neon atom. It enables us to study certain questions raised in recent picosecond photoionization experiments.[3]

In the second part of this study, molecular dynamics is used to study the thermodynamic and structural properties of single ions dissolved in bulk water as well as water clusters containing single ions. We show, contrary to our initial expectation, that the local structure and properties of ion–$(H_2O)_n$ clusters for $n = 31, 63$, and 215 are essentially independent of n and moreover are identical with what is found in the bulk-water system. This result indicates that the study of the structure of ion–$(H_2O)_n$ clusters may indeed shed light on the solvation of ions in bulk water. Thus this result tends to support the claim that recent molecular-beam studies[4] of small ion–water clusters are useful for the interpretation of phenomena in macroscopic liquids.

It is worth including a note of caution at this stage. In real solutions the ion–water interaction allows for a deformation of the water molecule as well as a polarization of the electronic distribution in both the ion and the H_2O molecules. In our model of the aqueous solution, the H_2O molecules are assumed to be rigid, and the ion–H_2O interaction is electrostatic and does not include electronic

polarization effects. Thus our conclusions, although accurate for the model (the ST2 model of H_2O), may not be entirely relevant to real water.

II. Molecular Model

The ST2 model of H_2O is adopted.[5] This model pictures the H_2O molecules as consisting of four point charges placed within a single Lennard-Jones sphere centered at the oxygen atom. Two positive charges are located at the positions of the H atoms, and two negative charges are located at the positions of the lone-pair orbitals. Two H_2O molecules, i and j, then interact according to the ST2 potential[5]

$$\phi_{i,j}^{W,W} =$$

$$4\epsilon_w\{(\sigma_W/r_{ij})^{12} - (\sigma_W/r_{ij})^6\} + \sum_{\alpha,\beta=1}^{4} (q_{\alpha j}q_{\beta i}/d_{\alpha\beta})S(r_{ij}) \quad (1)$$

where r_{ij} is the distance between the two oxygen atoms, and σ_W and ϵ_W are the parameters characterizing the Lennard-Jones (L-J) interaction. These are taken to be the neon value ($\epsilon_W = 5.260 \times 10^{-15}$ erg; $\sigma_W = 3.1$ Å). Throughout this paper all distances are reported in units of σ_W, and all energies in units of ϵ_W. All other properties are given in units reduced by these parameters. Thus time is given in units of $\tau = (M_W\sigma_W^2/\epsilon_W)^{1/2} = 2.34$ ps.

The second term in eq 1 represents the electrostatic energy of interaction between four charges (labeled α) on molecule i and the four charges (labeled β) on molecule j. The distance between charges α and β is denoted $d_{\alpha,\beta}$. A switching function, $S(r_{ij})$, is introduced[5]

$$S(r) = 0 \qquad r < R_1 = 0.6503$$

$$S(r) = (r - R_1)^2(3R_2 - R_1 - 2r)/$$
$$(R_2 - R_1)^3 \qquad R_1 \le r \le R_2 = 1.009 \quad (2)$$

$$S(r) = 1 \qquad r > R_2$$

(1) That there is a rather extensive literature on computer simulations of water is confirmed by a recent computer search which revealed that 128 papers have been published on this subject during the last three years. Thus we cite two general reviews: F. H. Stillinger, *Adv. Chem. Phys.*, **31**, 1 (1975); F. H. Stillinger, *Science*, **209**, 451 (1980).

(2) C. Pangali, M. Rao, and B. J. Berne, *J. Chem. Phys.*, **71**, 2975, 2982 (1979).

(3) K. Eisenthal, Ying Wang, M. K. Crawford, and M. J. McAuliffe, *Chem. Phys. Lett.*, **74**, 160 (1980).

(4) I. M. Tang and A. W. Castleman, Jr., *J. Chem. Phys.*, **57**, 3638 (1972); **60**, 3981 (1974); **62**, 4576 (1975); **65**, 4022 (1976).

(5) F. H. Stillinger and A. Rahman, *J. Chem. Phys.*, **60**, 1545 (1974).

†Name restored to Rao V. Mikkilineni. Bell Telephone Labs, Holmdale, NJ.

which cuts off the (otherwise divergent) electrostatic term at distances of close approach.

In all of the studies reported here the ion consists of a certain point charge, denoted q, embedded in the center of a Lennard-Jones neon sphere. The interaction between the ion and the jth ST2 H_2O molecule is

$$\phi_{A,j}^{ion,W} = 4\epsilon_W\{(\sigma_W/r_{Aj})^{12} - (\sigma_W/r_{Aj})^6\} \sum_{\beta=1}^{4} qq_\beta/d_{A\beta} \quad (3)$$

where r_{Aj} denotes the distance between the ion A and the O atom and $d_{A\beta}$ represents the distance between the ion and the βth charge on the H_2O molecule. The second term represents the electrostatic energy.

The total potential energy of a cluster containing N H_2O molecules and one ion is then

$$V = \sum_{i>j=1}^{N} \phi_{i,j}^{W,W} + \sum_{j=1}^{N} \phi_{A,j}^{ion,W} \quad (4)$$

Obviously, when $q = 0$, the potential represents the interaction between one Ne atom and N ST2 H_2O molecules.

III. Relaxation of Water Following Ionization

Molecular dynamics was used to simulate a periodic system containing a neon atom dissolved in 215 ST2 water molecules. In this "uniform system", the potential was spherically truncated at $r_c = 2.72$.[5] A complete description of the spherical cutoff and the effect of various boundary conditions on the structure of water is discussed elsewhere.[6] The equations of motion were integrated by using the SHAKE algorithm[7] with a time step of 0.005τ (1.175×10^{-15} s). The system was equilibrated at $T = 319$ K. After equilibration, this neutral system was run for 15000 time steps (17.63 ps). Thirty-one equally spaced phase points (500 time steps = 0.59 ps) were chosen from the neon run. For each of these states, the neon was charged to $q = +2$ (electronic charges), and a 250 time step trajectory (0.294 ps) was generated. These 31 independent relaxation trajectories constitute a nonequilibrium ensemble that can be used to determine ensemble averages.

In this paper we focus on the relaxation of the water structure around the cation (denoted A^{2+}). The radial distribution functions $\rho_{AO}(r,t)$ and $\rho_{AH}(r,t)$ give respectively the density of oxygen (O) and hydrogen (H) atoms at a distance r from the cation A^{2+}. These functions are formally defined as

$$\rho_{AB}(r,t) = \left\langle \frac{1}{4\pi r^2} \sum_B n_B^{-1}\delta(r - r_{AB}(t)) \right\rangle_{NE} \quad (5)$$

where $r_{AB}(t)$ is the distance between the ion (or neutral) A and an atom of type B (B = O or H), n_B is the number of atoms of type B in an H_2O molecule, and the sum goes over all atoms of type B in the system. The bracket indicates an average over the 31 relaxation trajectories, and the subscript denotes that this is a nonequilibrium ensemble. These functions are determined by counting the O and H atoms in a set of spherical shells surrounding the ion at a given time, dividing the results by the volumes of the shells, and averaging over the result for each of the 31 trajectories. In addition, the time-dependent running coordination number

$$N_{AO}(r) = 4\pi \int_0^R dr\, r^2 \rho_{AO}(r) \quad (6)$$

is determined.

(6) C. Pangali, M. Rao, and B. J. Berne, *Mol. Phys.*, **3**, 661 (1980).
(7) J. Ryckaert, G. Ciccotti, and H. J. C. Berendsen, *J. Comput. Phys.*, **23**, 327 (1977).
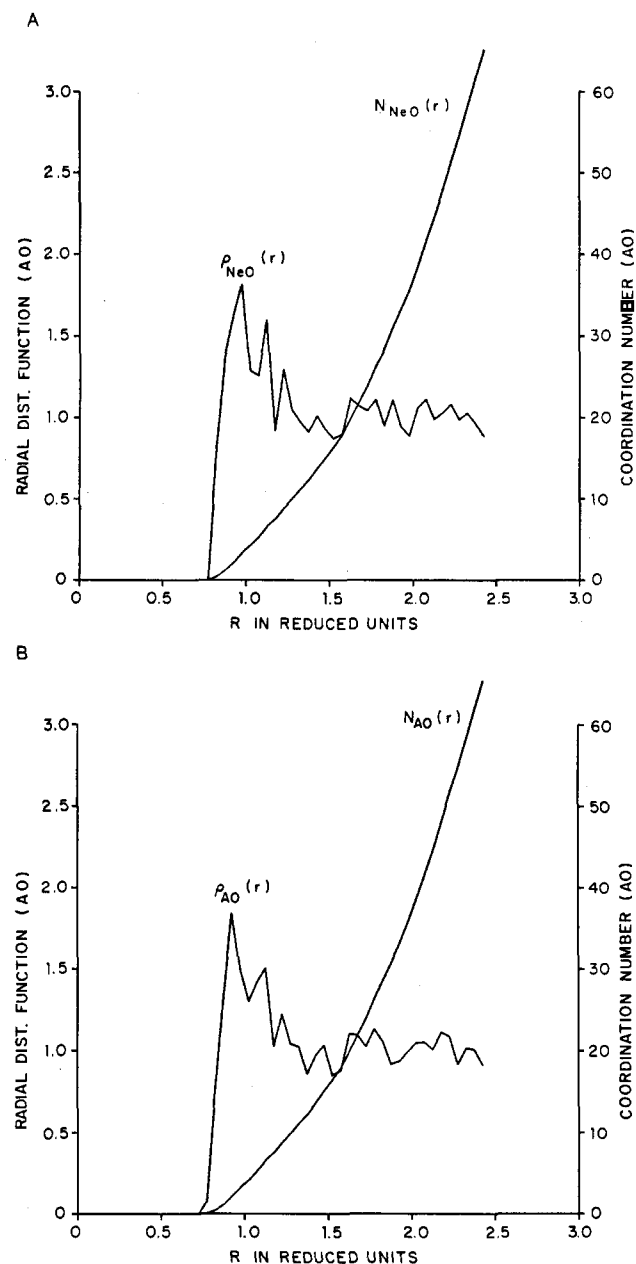
A structural property of considerable interest is the radial component of the dipole moment (or polarization). Because the system has spherical symmetry about the dissolved ion, there will be no net electrical polarization. Nevertheless the radial component of the dipole moment will not average to zero. Thus we determine the radial dipole distribution function

$$g_\mu(r,t) = \left\langle \frac{1}{4\pi r^2} \sum_{\alpha=1}^{N} (\mu_\alpha \cdot \hat{\mathbf{r}}_{A\alpha}(t))\, \delta(r - r_{A\alpha}(t)) \right\rangle_{NE} \quad (7)$$

Here μ_α, $\hat{\mathbf{r}}_{A\alpha}$, and $r_{A\alpha}$ are respectively the dipole moment of the αth water molecule, the unit vector pointing from the ion to the oxygen atom on the αth water molecule, and the distance from the ion to the oxygen atom on the αth water molecule. The radial dipole distribution is determined by summing the quantity $\mu_\alpha \cdot \hat{\mathbf{r}}_{A\alpha}$ in spherical shells centered on the charge and dividing the result by the number of water molecules in the shells.

The electric field emanating from the neon atom after it is charged gives rise to forces and torques on the neighboring H_2O molecules and leads to linear and angular acceleration. This leads to a heating up of the region around the ion. It is useful to determine how the local temperature $T(r,t)$ varies with distance from the ion and time. The total kinetic energy of the αth rigid H_2O molecule is

$$(KE)_\alpha = \sum_{B\in\alpha} \frac{P_B^2}{2M_B} \quad (8)$$

where the sum goes over all B atoms (B = O, H) in this αth molecule. The local temperature is then defined as

$$3kT(r,t) = \left\langle \sum_{\alpha\in\Delta r} (KE)_\alpha / \sum_{\alpha\in\Delta r} 1 \right\rangle_{NE} \quad (9)$$

This is simply the mean kinetic energy per H_2O molecule at time t in the shell Δr located at radius r. Since the kinetic energy $(KE)_\alpha$ can be decomposed into a translational and rotational contribution, it follows that

$$T(r,t) = \frac{1}{2}[T^R(r,t) + T^T(r,t)] \quad (10)$$

where $T^R(r,t)$ and $T^T(r,t)$ are the rotational and translational temperatures. The translational temperature can be determined from the kinetic energy of the center of mass (KE of COM) of each molecule by using eq 11. Thus

$$\frac{3}{2}kT^T(r,t) = \left\langle \sum_{\alpha\in\Delta r} (KE\ of\ COM)_\alpha / \sum_{\alpha\in\Delta r} 1 \right\rangle_{NE} \quad (11)$$

a determination of $T^T(r,t)$ and $T(r,t)$ gives after substitution into eq 10 the value of the rotational temperature, $T^R(r,t)$.

Because each of the 31 relaxation trajectories is of length (0.294 ps), the water molecules have not completely relaxed to the equilibrium structure around A^{2+}. To study the full relaxation would be prohibitively expensive—requiring many trajectories each consisting of some 10000 time steps (11.7 ps). Despite this we can learn much about the short time structural relaxation of H_2O.

It is important to determine whether the 31 relaxation trajectories suffice for an accurate determination of the structural properties of relaxing fluid. Since the initial states are selected from the 15000-step equilibrium run of neon in H_2O by choosing the state after every 500th step (0.59 ps), it is expected that the fluid configurations represented by these 31 states will be reasonably uncorrelated. These 31 initial states are used to determine the neon-oxygen radial distribution function and the corresponding running coordination number. The results are presented in Figure 1A. In Figure 1B the neon–oxygen radial dis-

A

B

Figure 1. Radial distribution function, $\rho_{NeO}(r)$, of oxygen atoms around neon and the corresponding running coordination number at a temperature of 319 K: (A) averaged over 600 equally spaced configurations; (B) averaged over 31 equally spaced configurations.

tribution is determined by using every 25th state of the 15 000-step run (600 states in all). Comparison of parts A and B of Figure 1 shows that the 31 initial states give as accurate a radial distribution as one determined on the basis of many more states. Clearly the accuracy depends on the number of statistically independent smaplings. If τ_R is the configurational correlation time for $\rho_{AO}(r)$, then the number of independent samplings is proportional to T/τ_R and the corresponding error is proportional to $\pm(\tau_R/T)^{1/2}$. The agreement between parts A and B of Figure 1 implies that $\tau_R > 250$ steps. This agreement leads us to believe that our study of relaxation using only 31 trajectories is significant.

Figure 1, A and B, is very similar to that obtained by Geiger et al.[8] in a previous study of hydrophobic hydration of Ne in ST2 H_2O. They pointed out that the hydration
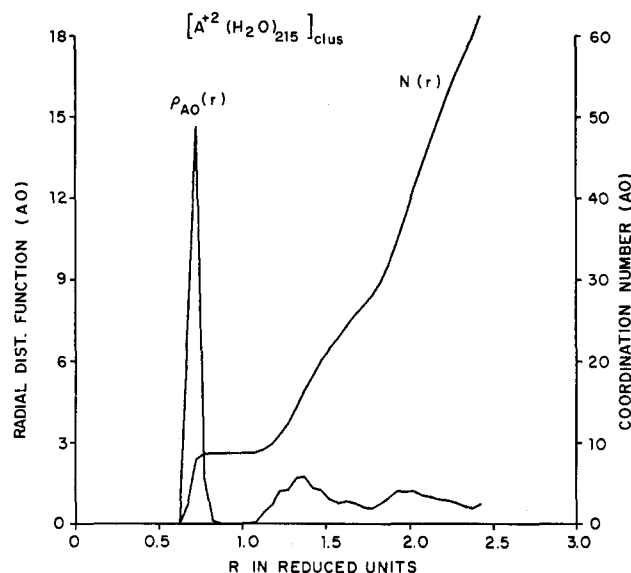
(8) A. Geiger, A. Rahman, and F. H. Stillinger, *J. Chem. Phys.*, 70, 263 (1979).

Figure 2. Radial distribution function, $\rho_{AO}(r)$, and the coordination number, $N_{AO}(r)$, of oxygen atoms around a divalent cation A^{2+} at a temperature of 309 K.

shell of Ne contains $\sim$14 H_2O molecules. They noted a barely perceptible shoulder in $\rho_{Ne-O}(r)$ between 3.9 and 4.8 Å and suggested that the entire hydration shell splits into two subshells containing eight and six molecules, respectively. This is consistent with a clathrate-like structure around Ne. It is important to note that, because Figure 1, A and B, has larger error bars than those of Geiger et al., this shoulder is not observed; nevertheless, the running coordination number does give a hydration shell of $\sim$14 H_2O molecules.

At time $t = 0$ the neutral neon (A^0) is charged to +2 becoming a cation A^{2+}. Although we are primarily concerned with structural relaxation, it is important to ascertain the equilibrium structure of water around A^{2+}, that is, the properties of the fully relaxed system. This is discussed in greater detail in the next section. Here it suffices to discuss the A^{2+}-O radial distribution and running coordination number given in Figure 2. It should be noted that the radial distribution has a narrow peak centered considerably closer than the Lennard-Jones contact distance of $R = 0.91$ (2.82 Å) for the case of Ne-oxygen (cf. Figure 1A). Moreover, the peak is very narrow. This springs from the very strong electrostatic interaction between the ion and the charges on ST2 water. The running coordination number rises steeply at $R = 0.72$ (2.02 Å) to a value of 8.75 and remains at this value until $R = 1.08$ (3.02 Å). This behavior suggests that the ion is strongly solvated as $A^{2+}(H_2O)_{8.75}$. Thus, upon ionization the charged species becomes solvated. It is our purpose to study the kinetics of such a process.

Precisely how the radial distribution functions, $\rho_{AO}(r,t)$, $\rho_{AH}(r,t)$, and $g_\mu(r,t)$, vary with time after ionization is indicated in Figures 3–5. The bottom curves in each of these figures correspond to the fluid at a time equal to 10 time steps (1.175 × 10^{-3} ps) after ionization, and, going up from the bottom curve, each subsequent curve represents 10 steps (1.175 × 10^{-3} ps) of evolution. The whole set of curves represents the structural relaxation of the system for 500 time steps (0.588 ps) after ionization. The zero for each curve is given by its ordinate at its extreme left. Thus by scanning from bottom to top, these plots give the structural relaxation.

Figure 3 shows that both the first peak of the $\rho_{AO}(r)$ and the distance of closest approach of the oxygen to the ion moves in after ionization. The position of the first peak
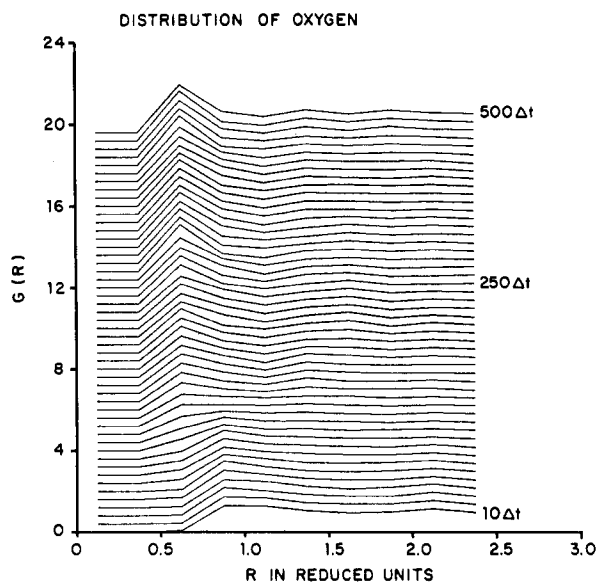
DISTRIBUTION OF OXYGEN

Figure 3. Radial distribution function, $G(R) \equiv \rho_{AO}(r, t)$ of oxygen atoms around A^{2+}. The bottom curve corresponds to $10\Delta t$ (1.175×10^{-3} ps) after ionization. Each curve gives the structure after 10 steps elapsed time.
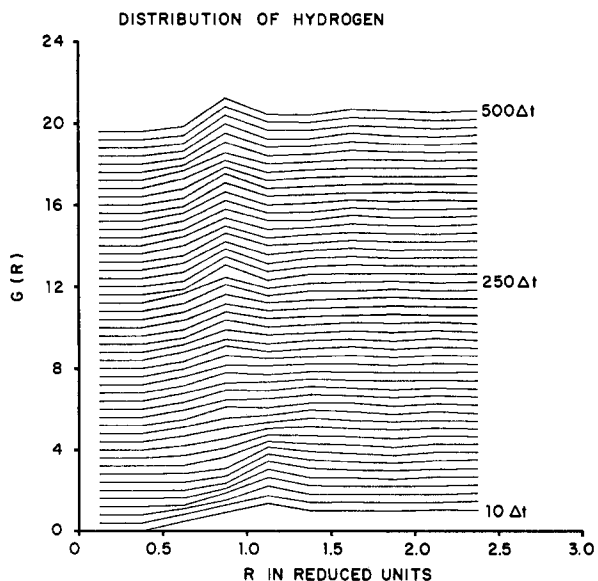
DISTRIBUTION OF HYDROGEN

Figure 4. Radial distribution function $G(R) = \rho_{AH}(r, t)$ of hydrogen atoms around A^{2+}. The sequence of curves is as described in the caption of Figure 3.

seems to remain at $R \simeq 0.8$ (2.48 Å) for 100 time steps (0.118 ps) and then, in a relatively short period (50 time steps), to "jump" to $R \simeq 0.6$. The peak remains at this point for the remaining relaxation. The same is true for the distance of closest approach of oxygen to the ion. Thus ionization is not followed by continuous electrostriction. It should be noted that for large R ($R \geq 1.4$ (4.34 Å)), the number density of oxygen atoms does not change at all during the total run (0.5 ps).

Figure 3 shows that the evolution of the ion–oxygen radial distribution function can be described as follows. Initially no oxygen atoms are found closer to the ion (neon) than $R = 0.775$ (2.4 Å). As time progresses, however, the oxygen atoms move closer to the ion but get no closer than $R \approx 0.6$ (1.86 Å). The first peak of the radial distribution function, ρ_{AO}, moves in, and the running coordination number increases, indicating that the ion is indeed becoming solvated. As was already noted, this electrostriction is accompanied by a "heating up" to be described mo-
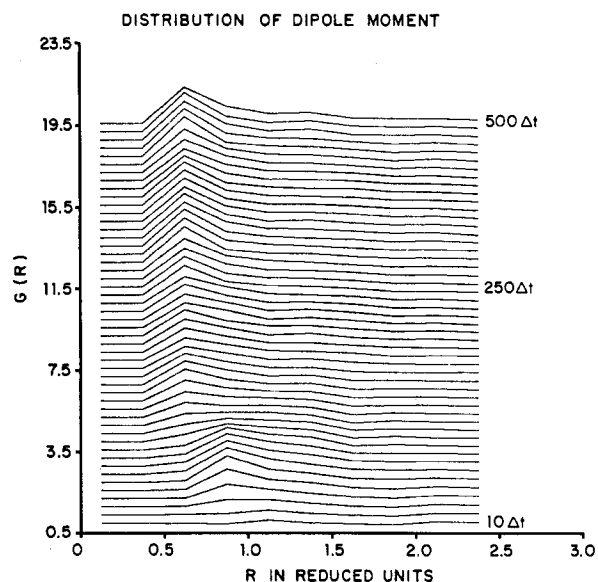
DISTRIBUTION OF DIPOLE MOMENT

Figure 5. Distribution $G(R) = g(r, t)$ of the radial component of the dipole moment of H_2O (cf. eq 7) around A^{2+}. The sequence of curves is as described in the caption to Figure 3.
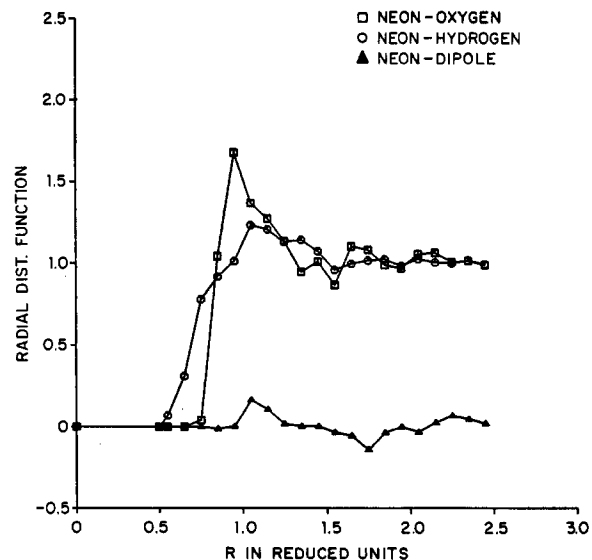

Figure 6. Equilibrium structure of H_2O around a neon atom: (□) the radial distribution of oxygen; (O) the radial distribution of hydrogen; (△) the distribution of the radial component of the H_2O dipole around a neon atom at $T = 319$ K in bulk H_2O.

mentarily. It is because of this local heating that the ρ_{AO} radial distribution at the top of Figure 3 is much broader than the low-temperature ($T = 319$ K) equilibrium radial distribution given in Figure 2.

The evolution of the radial distribution of hydrogen atoms around the ion is given in Figure 4. Comparison of the bottom curves with $\rho_{NeH}(r)$ given in Figure 6 shows that immediately after ionization the $\rho_{AH}(r)$ peak is displaced slightly to the right of where it was with respect to neutral neon, indicating that the protons in the H_2O molecules have rotated away from the positive ion taking between 25 and 50 time steps (0.03–0.06 ps). After considerable time (~0.118 ps) the $\rho_{AH}(r)$ peak moves in toward the ion. This happens in ~0.06 ps and can be attributed to the electrostriction mentioned in connection with the behavior of $\rho_{AO}(r)$. The large positive charge on A^{2+} attracts the now properly oriented water dipoles. Thus it appears that, because the moment of inertia of H_2O is small, the H_2O molecules rapidly rotate away from the positively charged ion and are then attracted toward it.
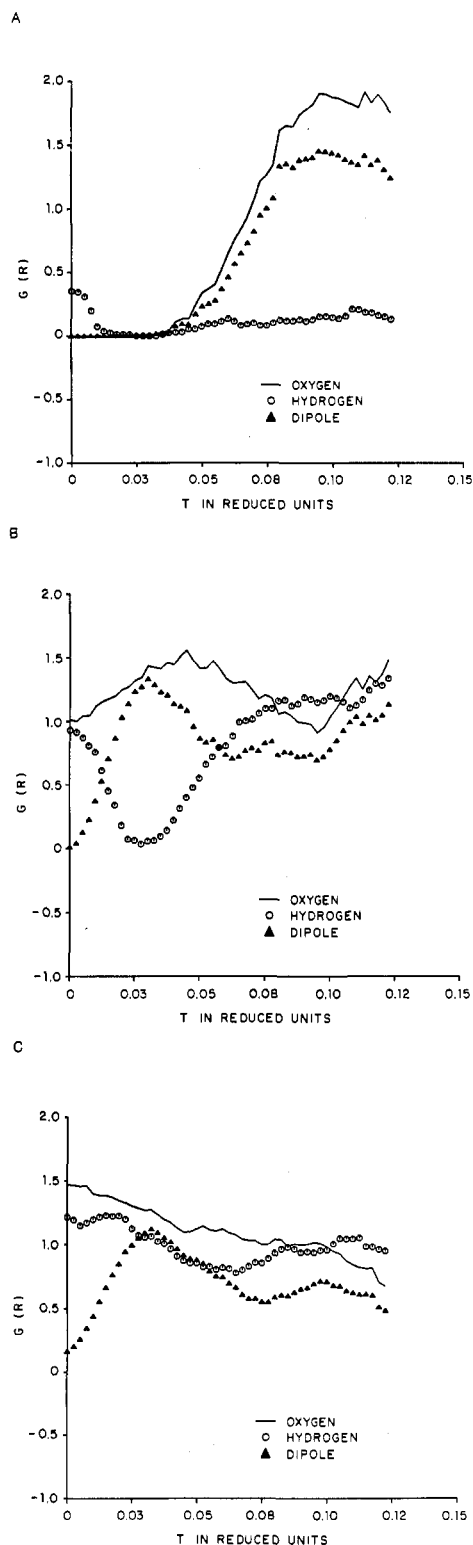
A

B

C

Figure 7. Relaxation of the structure of water around the A^{2+} ion as a function of time elapsed since ionization: (—) $\rho_{AO}(r,t)$; (○) $\rho_{AH}(r,t)$; (△) $g_\mu(r,t)$. (A) Relaxation of the molecules located between 1.55 and 2.33 Å. (B) Relaxation of the molecules located between 2.33 and 3.1 Å. (C) Relaxation of the molecules located between 3.1 and 3.35 Å.

The time evolution of the radial component of the dipole moment (cf. eq 7) is given in Figure 5. It should be noted that this function is essentially zero before ionization (see Figure 6). After ionization Figure 5 shows that a peak develops in $g_\mu(r,t)$ at the same position as observed in $\rho_{AO}(r,t)$ (see Figure 6). This means that the water molecules in the first peak of the charged ion rotate after ionization such that these protons are pointing away from the
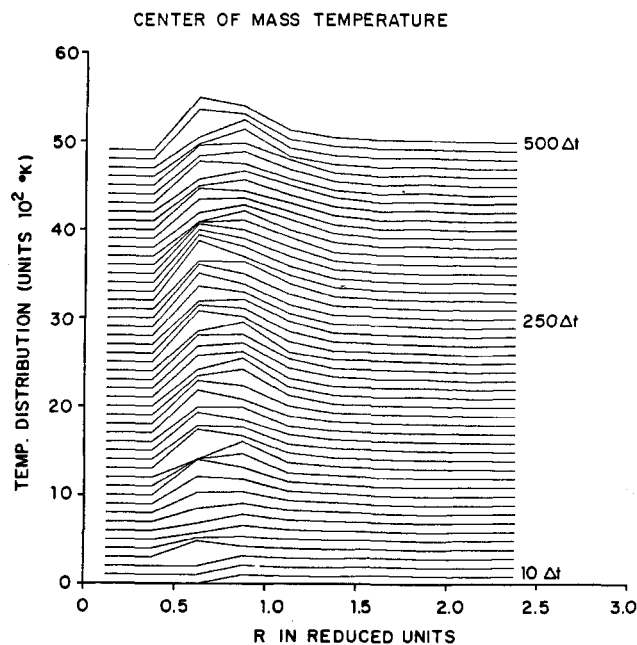
CENTER OF MASS TEMPERATURE

Figure 8. Radial dependence of the translational temperature of the water molecules around an A^{2+} ion and its dependence on elapsed time after ionization. The sequence of curves is as described in caption 3.

positive ion. This happens in ~50 time steps (0.06 ps). After 100 time steps the peak in $g_\mu(t)$ shifts in just as the peak $\rho_{AO}(r,t)$ does. This is due to electrostriction and occurs in ~100 time steps. Thus once again we see that the neighboring H_2O molecules first rotationally and then translationally relax. Needless to say, the precise time dependence can be rather complicated, but ball-park estimates of the relaxation times are possible.

The time dependence of $\rho_{AO}(r,t)$, $\rho_{AH}(r,t)$, and $g_\mu(r,t)$ as a function of time for fixed values of r are given in Figure 7A–C. The mesh used for the determination of these radial distributions is $\Delta r = 0.25$ (0.775 Å), and, because a longer time period is studied, only 12 relaxation trajectories are used here. A review of these figures supports our previous comments. For example, in Figure 7A, we see that during the time from 0 to 0.07 ps after ionization no O atoms are found between $R = 0.5$ (1.55 Å) and $R = 0.750$ (2.3 Å). During this time H atoms originally in this region move out. After 0.07 ps the O atoms move into this region followed by H atoms. This is consistent with our view that the H_2O molecules nearest the neon first reorient such that their protons point away from the ion and only then move in toward the ion. Figure 7A shows that this reorientation takes place very rapidly in ~0.05 ps. In the next shell, $0.75 \le r \le 1.0$, shown in Figure 7B, during the first 0.07 ps O atoms move into the shell (from the next most distant shell (see Figure 7C), and once again the H atoms initially in the shell rapidly move out (away from the ion). After this initial period, the number of oxygen atoms decreases, moving into the closer shell (see Figure 7A). Meanwhile, the number of H atoms increases.

After ionization, the H_2O molecules near the ion are exposed to strong electrostatic forces and torques. Those further away are screened by the closer H_2O molecules. Thus the H_2O molecules close to the ion will be accelerated to very high linear and angular velocities and thereby will "heat up". The radial and time dependences of the translational ($T^T(r,t)$), rotational ($T^R(r,t)$), and total ($T(r,t)$) temperatures are given in Figures 8–10. Again time increases from bottom curve to top curve in increments of 10 time steps. The bottommost curve corresponds to 10
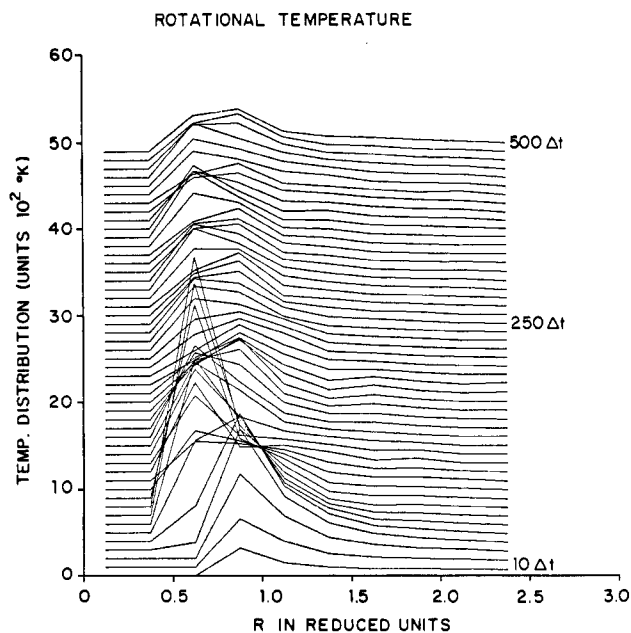
ROTATIONAL TEMPERATURE

Figure 9. Radial dependence of the rotational temperature of the water molecules around an A^{2+} ion and its dependence on elapsed time after ionization. The sequence of curves is as described in caption 3.
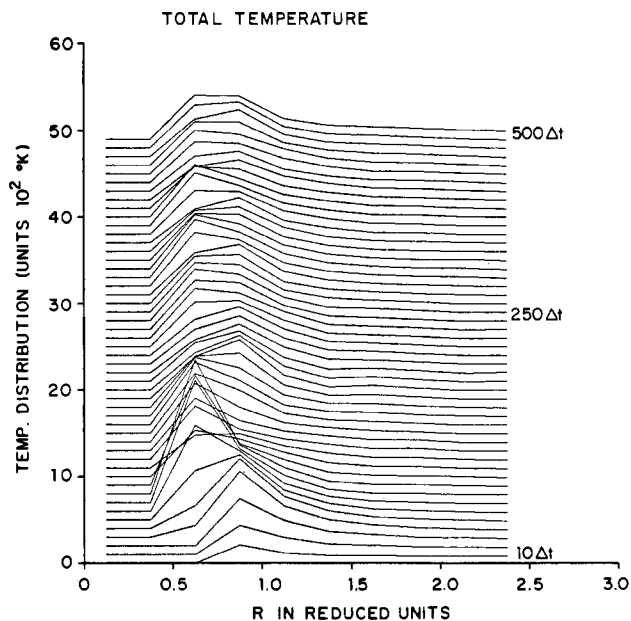
TOTAL TEMPERATURE

Figure 10. Radial distribution of the total temperature of the water molecules around an A^{2+} ion and its dependence on elapsed time after ionization. The sequence of curves is as described in caption 3.

time steps (0.0118 ps) after ionization. For R → 0, the temperature is zero because there are no H_2O molecules in this region. Figures 8–10 show that ionization creates a "local hot spot". During the entire 0.59-ps run, this hot spot stays fairly localized, an observation that can be rationalized on the basis of the thermal conductance and sound speed of the system.

In Figure 8 we see that the peak in the translational temperature essentially follows that of $\rho_{AO}(r,t)$ given in Figure 3 with an accompanying diffusion to larger distances at long times. This means that velocity relaxation is much faster than structural relaxation. In Figure 9, it should be noted that the rotational temperature rises very rapidly at the position of the first peak in $\rho_{AO}(r,t)$ in Figure 3 and then moves in following the ρ_{AO} peak. This is again consistent with our interpretation that initially the neighboring H_2O molecules reorient before electrostriction

takes place. The subsequent evolution of $T^R(r,t)$ shows that it equilibrates with the local translational temperature. The behavior of the total local temperature is given in Figure 10.

The picture that emerges is that the relaxation of the water molecules close to the ion takes place in a local hot spot of very high temperature. This hot spot only very slowly diffuses away by ordinary thermal conduction and sound propagation. Thus there is a very rapid relaxation followed by a very slow one. It would be entirely incorrect to interpret this relaxation in terms of orientational and translational correlation times determined on the basis of fluctuation spectroscopy on water at the temperature preceding ionization. These results strongly suggest that the water molecules in the first few solvent shells relax much faster than those farther away from the ion.

Rahman and Stillinger[9] in their molecular dynamics study of H_2O have determined values for the correlation time, τ_1, of the self-dipolar-correlation function. They find that $\tau_1 = 5.6$ ps at 307 K and $\tau_1 = 0.34$ ps at 587 K. When neon is ionized at 319 K, we find that the protons relax on a time scale of 0.07 ps. Clearly our result cannot be explained on the basis of $\tau_1 \approx 5.6$ ps. Nevertheless, given the very strong temperature dependence of τ_1, it is conceivable that the rapid tumbling observed after ionization can be explained by the value of τ_1 at a temperature ($T_R \approx 1200$ K) corresponding to the local rotational temperature. In point of fact, the rapid tumbling is due to the unscreened torque seen by the water molecules closest to the charge. Moreover, it should be clear that any theoretical attempt to model the dynamics of the solvent immediately following ionization must deal with the strong temperature gradients involved. The ordinary Smulochowski equation will simply not suffice for a description of this phenomenon.

IV. Structure Equilibrium of Water around an Ion

In this section, molecular dynamics is used to study the structural properties of single ions dissolved in bulk water as well as in water clusters. Several studies of solvation of ions already exist.[10] The thrust of this study is to provide some insight into the question as to how large a cluster must be before its structural properties are the same as those in the bulk fluid. In this section, molecular dynamics is performed with the same time steps and parameters as those described in sections II and III.

We adopt the notation $[A^Z(H_2O)_n]$ to denote an ion A with charge Z (=0, +1, −1, +2) (in units of the electronic charge) dissolved in n ST2 H_2O molecules. In all systems discussed below, A denotes a spherical particle with the same L-J parameters (σ_w, ϵ_w) used in the ST2 interaction. A can thus be regarded as a "charged neon atom". The symbol $[A^Z(H_2O)_n]_{unif}$ denotes a system in which periodic boundary conditions are used in conjunction with a spherical cutoff $r_c = 2.72$. This system has no free surfaces and is therefore to be regarded as a uniform system. The uniform systems discussed here all have $n = 215$. Three such systems have been studied, $[A^0(H_2O)_{215}]_{unif}$ and $[A^{1\pm}(H_2O)_{215}]_{unif}$. Each of these systems is first equilibrated and then run for M steps. The temperatures and numbers of steps used are summarized in Table I.

(9) F. H. Stillinger and A. Rahman, *J. Chem. Phys.*, **57**, 1281 (1972).
(10) See, for example: C. L. Briant and J. J. Burton, *J. Chem. Phys.*, **64**, 2888 (1976); F. F. Abraham and M. Mruzik, *Discuss. Faraday Soc.*, **61**, 34 (1976); M. Mruzik, *Chem. Phys. Lett.*, **48**, 171 (1977); E. Clementi, G. Corongiu, B. Joensson, and S. Romano, *J. Chem. Phys.*, **72**, 260 (1980); F. Abraham, *ibid.*, **61**, 2221 (1974); K. Binder, *ibid.*, **63**, 2265 (1975); M. Mruzik, F. Abraham, D. Schreiber, and G. M. Pound, *ibid.*, **64**, 481 (1976).

TABLE I

	no. of steps M	temp, K	total energy,[a] ϵ_ω	pot. energy total (ion-H_2O)
$[A°(H_2O)_{215}]_{unif}$	15000	319	-103.2	
$[A^{1+}(H_2O)_{215}]_{unif}$	5000	336	-101.8	-131.4
$[A^{1+}(H_2O)_{215}]_{clus}$	5000	326	-87.3	-112.6
$[A^{1+}(H_2O)_{63}]_{clus}$	5000	292	-100.0	-122.8
$[A^{1+}(H_2O)_{31}]_{clus}$	10000	281	-109.4	-134.3
$[A^1(H_2O)_{215}]_{unif}$	5000	328	-104.3	-132.7
$[A^{1-}(H_2O)_{215}]_{clus}$	5000	334	-87.1	-112.4
$[A^{1-}(H_2O)_{63}]_{clus}$	5000	320	-99.7	-124.7
$[A^{2+}(H_2O)_{215}]_{clus}$	6000	309	-111.0	-135.0

[a] Total energy is equal to potential plus kinetic energy per molecule. [b] Only includes Coulomb interaction (per H_2O molecule) between ion and H_2O.
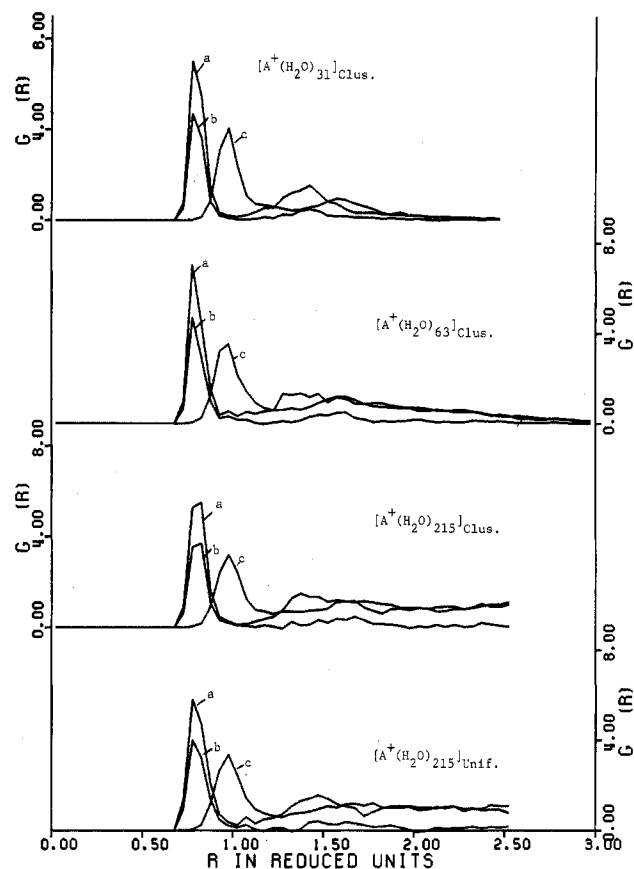

Figure 11. Equilibrium structure of water around a monovalent cation in different environments is indicated. Curve a gives the radial distribution of oxygen, $\rho_{AO}(r)$; curve b gives the radial distribution of hydrogen, $\rho_{AH}(r)$; curve c gives the distribution g(r) of the radial component of the dipole moment around A^+.

The last microscopic state generated for the two systems $[A^{1\pm}(H_2O)_{215}]_{unif}$ are used as initial states for the following simulation. First the periodic boundary conditions are removed. The two systems then become cubic clusters, one with an A^+ and the other with an A^- at the center. These systems have free surfaces. Second, the spherically truncated potentials are replaced by untruncated potentials. Molecular dynamic runs are then used to equilibrate the system at particular temperatures (cf. Table I), and runs of length M are generated. The two systems produced in this way are denoted $[A^\pm(H_2O)_{215}]_{clus}$. To produce $[A^{2+}(H_2O)_{215}]_{clus}$ one charges the system containing the A^+ ion to A^{2+} and an equilibrium run of M steps (cf. Table I) is generated.
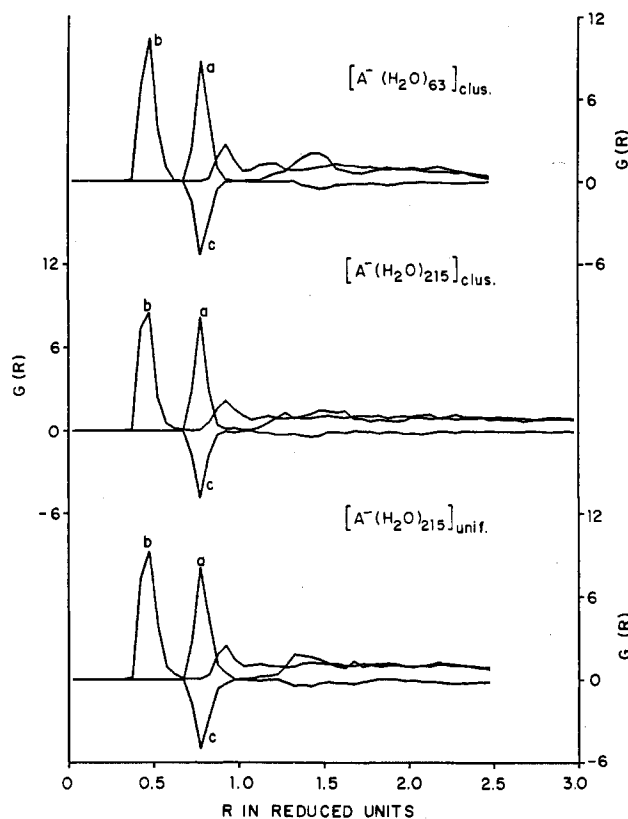

Figure 12. Equilibrium structure of water around a monovalent anion. Curves a–c correspond to the radial distribution functions described in Figure 11.
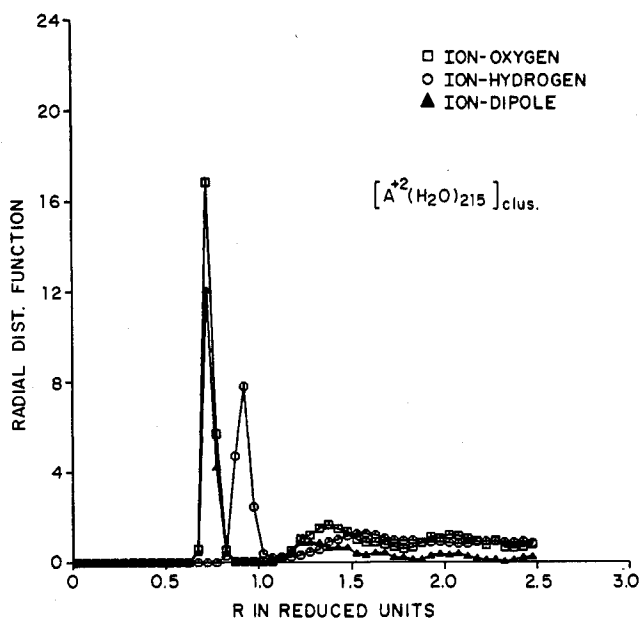

Figure 13. Equilibrium structure of water around a divalent cation: (□) ion–oxygen, (O) ion–hydrogen, and (Δ) ion–dipolar radial distributions.

To simulate clusters $[A^+(H_2O)_{63}]_{clus}$ and $[A^-(H_2O)_{63}]_{clus}$ the last states of $[A^\pm(H_2O)_{215}]_{clus}$ were chosen, and all but the 63 nearest neighbors of the A^+ and A^- ions were removed. In like manner the cluster $[A^{1+}(H_2O)_{31}]_{clus}$ was produced. These systems were then used to generate equilibrium trajectories consisting of M steps (cf. Table I).

The properties determined are the radial distributions $\rho_{AO}(r)$, $\rho_{AH}(r)$, and $g_\mu(r)$ and the running coordination number $N_{AO}(r)$. These quantities are determined differently than in section III. Here the atoms (or radial dipoles)
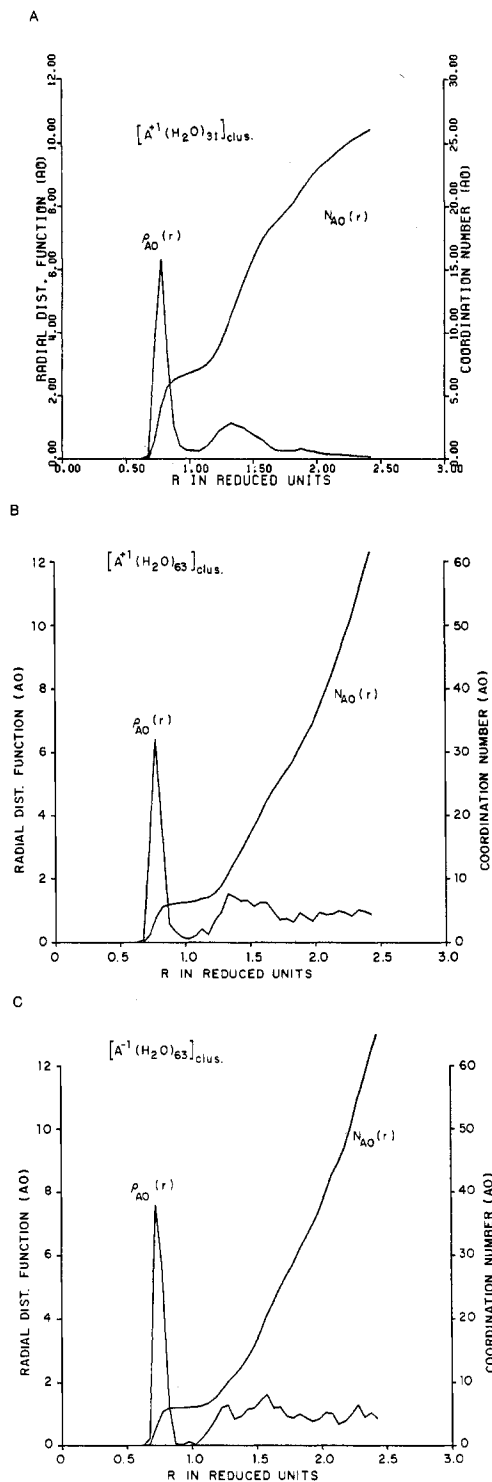
Figure 14. (A) Radial distribution function, $\rho_{AO}(r)$, and the running coordination number, $N_{AO}(r)$, of oxygen atoms around a monovalent cation, $[A^+(H_2O)_{31}]_{clus}$. (B) Radial distribution function, $\rho_{AO}(r)$, and the running coordination number, $N_{AO}(r)$, of oxygen atoms around a monovalent cation, $[A^+(H_2O)_{63}]_{clus}$. (C) Radial distribution function, $\rho_{AO}(r)$, and the running coordination number, $N_{AO}(r)$, of oxygen atoms around a monovalent anion, $[A^-(H_2O)_{63}]_{clus}$.

are counted in each shell (of width $\Delta r = 0.05$ (0.155 Å)) after every 10 time steps and averaged over an equilibrium run of length M (see Table I).

In Figures 11–13, these properties are given respectively for the hydrated A^+, A^-, and A^{2+} ions. In Figure 14A–C,

the running coordination number $N_{AO}(r)$ is given for $[A^{\pm}(H_2O)_{63}$.

Several features of these curves are noteworthy:

(a) For each ion (A^+ and A^-) the radial distribution (cf. Figures 11 and 12) are essentially identical for the 31-H_2O, 63-H_2O, and 215-H_2O clusters and the 215-H_2O uniform system. Small differences can be perceived for the 31-H_2O cluster only at long distances.

(b) The running coordination numbers $N_{AO}(r)$ indicate (cf. Figure 14A–C) that there are six H_2O molecules in the first hydration shell of A^+ and A^-. These data are consistent with an octahedral hydration shell. This should be compared with what is found for $[A^{2+}(H_2O)_{215}]_{clus}$ in Figure 2. The ion A^{2+} appears to have a hydration shell consisting, on the average, of 8.75 H_2O molecules. If the coordination number were 8.0, we could assume that A^{2+} has a simple cubic hydration shell. That $N_{AO}(r)$ has a very well-defined plateau at 8.75 indicates that two or more relatively long-lived hydration shells may contribute sequentially to structures. It is completely possible that the run is not long compared to the relaxation times of these shells.

(c) The ion strongly polarizes the water molecules so that for A^+ and A^{2+} the dipoles point away from the ion whereas for A^- the dipoles point toward the ion entirely as expected. This behavior is indicated by the positive and negative peaks in $g_\mu(r)$ corresponding to A^+ and A^-, respectively. In all cases $g_\mu(r)$ exhibits a very well-defined peak at precisely the same position as the first peak $\rho_A(r)$. In addition, in all cases $g_\mu(r)$ has a very small tail. This means that the hydration shell of the ion very effectively screens out the field of the ion and gives rise to very little radial polarization beyond the first shell.

These observations lead us to conclude that the local structure of H_2O around ions are essentially independent of the boundary conditions used in the simulation. It is entirely possible to make accurate studies of solvation effects using relatively small clusters. This simplifies the simulation of chemically interesting phenomena. Recent simulations of solvation around proteins and dipeptides incorporate only a small number of H_2O molecules. Despite our initial doubts about the validity of this approach, our study shows that, if there are a sufficient number of H_2O molecules to give next nearest neighbors to various groups on the proteins, there is reason to believe that these results are valid.

In recent years, nozzle beam techniques have been used to study the properties of ions embedded in clusters of H_2O molecules. There has been some question as to how large a cluster must be before it displays the properties of a macroscopic sample. These experiments do not give the kind of detailed structural information that we present here. They do, however, give thermodynamic properties as a function of cluster sizes. We have shown here that clusters containing as few as 31 H_2O molecules ($R = 1.75$) (5.43 Å) already give local structural information about macroscopic samples (cf. Figures 12–14). In contrast to the studies on the structure of pure water,[6] these studies on the structure of water around an ion do not exhibit marked differences with the size of the sample. Thus our study elucidates the special role that ions play in the solvation process.